Online ISSN 1848-3380, Print ISSN 0005-1144
ATKAFF 57(1), 163–172(2016)

Chams-Eddine Feraga, Abdallah Bouldjedri

Performance of a Photovoltaic Pumping System Driven by a Single Phase Induction Motor Connected to a Photovoltaic Generator

DOI 10.7305/automatika.2016.07.851
UDK [621.313.333.025.1-531-533.7:621.383.51]:621.67.052

Original scientific paper

Solar energy is one of the most widely used renewable sources in the world. This explains the interest shown by researchers on the improvement of the quality and performances of this renewable source. The availability of low-cost solar cells increases the interest and needs in photovoltaic (PV) system applications following standard of living improvements. Nowadays, water pumping systems powered by solar-cell generators are one of the most important applications. In fact three phase induction motor fed by PVG is well known in literature, while the single phase induction motor for low power application used widely in domestic utility has never been investigated. In this paper the performances of a single phase induction motor (SPIM) connected to a photovoltaic generator (PVG) through an inverter are analyzed. Firstly, the mathematical model of the suggested structure is developed. Secondly, the concept of the Indirect Rotor-Field-Oriented Control (IRFOC) techniques is used to pilot the working of the single phase induction motor coupled with the centrifugal pump. Then, the chosen maximum power point tracking algorithm MPPT adjust pump operation to meet the desired water flow and pressure conditions. The proposed approach has the advantage no use the DC/DC converter, reduced size, low cost. This results in much higher overall system operating efficiencies. Finally, Simulation results show the effectiveness and feasibility of the suggested approach.

Key words: single-phase induction motor, field oriented control, photovoltaic generator, pumping, modeling, optimization, efficiency

Perfomanse fotonaponskog sustava pumpanja pogonjenog jednofaznim indukcijskim motorom spojenim na fotonaponski generator. Solarna energija je jedna od najkorištenijh oblika obnovljivih izvora energije u svijetu. To objašnjava interes istraživača za poboljšanjem kvalitete i performansi ovog obnovljivog izvora. Dostupnost jeftinih solarnih ćelija povećava interes i potrebu za aplikacijama fotonaponskih (PV) sustava prateći rast kvalitete životnih uvjeta. Danas, jedna od najvažnijih aplikacija je u sustavima za pumpanje vode. Zapravo, trofazni indukcijski motor kojeg pogoni PVG je dobro poznat u literaturi, dok jednofazni indukcijski motor koji se koristi u energetski nezahtjevnim sustavima kao što su kućanski aparati nikad nije istraživan. U ovom radu se analiziraju performanse jednofaznog indukcijskog motora (SPIM) spojenog na fotonaponski generator (PVG) pomoću invertera. Prvo je razvijen matematički model predloženog sustava. Potom je koncept indirektnog upravljanja orijentacijom-polja-rotora (IRFOC) korišten za upravljanje jednofaznim indukcijskim motorom spojenim s centrifugalnom pumpom. Zatim je iskorišten algoritam praćenja točke najveće snage (MPPT) za prilagodbu rada pumpe na zahtjevane protočne i tlačne uvjete. Predloženi pristup ima prednost korištenja DC/DC konvertera, smanjene veličine i niske cijene. Rezultat je mnogo veća efikasnost rada cjelokupnog sustava. Konačno, simulacijski rezultati pokazuju efektivnost i izvedivost predloženog pristupa.

Ključne riječi: jednofazni indukcijski motor, kontrola orijentacije polja, fotonaponski generatir, pumpanje, modeliranje, optimizacija, efikasnost

1 INTRODUCTION

The development of renewable energy has been an increasingly critical topic in the 21^{st} century with the growing problem of global warming and other environmental issues. With greater research, alternative renewable sources such as wind, water, geothermal and solar energy, have become increasingly important for electric power generation. Solar energy is one of clean renewable energy and represents an alternative to conventional energy sources that produce toxic waste or pollutants. This source of energy can be used for different applications, for example to charge a battery, to feed the grid network and for a standalone PV pumping system.

Water resources are essential for satisfying human needs, social and economic development, protecting health, ensuring food production, energy, the restoration of ecosystems,and also for sustainable development. However, in many arid countries, people are affected by water shortages and do not have sufficient drinking water, therefore there is a great and urgent need to supply drinking water. Remote water pumping systems are a key component in meeting this need where no grid system is available.

Water pumps are driven by various types of motors. This explains the interest shown by researchers on the improvement of the quality and performances of these photovoltaic pumping systems. In general, DC motors are used because they are highly efficient and can be directly coupled with a PV module or array[1-2-3]. A number of existing operational pumping systems have shown that these schemes suffer from maintenance problems. To overcome this drawback, different AC motors have been used in [4-5-6-7-8-9-10-11].During these last years, many research laboratories focused on the variable-speed drives, especially for the Single-Phase Induction Motor (SPIM), and important renovations have been achieved on this theme [12-13-14-15].

In this work, the photovoltaic water pumping system is constituted by a photovoltaic generator PVG, a condenser, a PWM inverter, a single phase induction motor and a centrifugal pump. In order to force the PVG to operate at its maximum power point under different solar illumination conditions, we develop a maximum power point tracking algorithm MPPT which calculates the reference speed of the SPIM versus the solar illumination. The induction motor pump is controlled by the field oriented technique; it has been proposed to ensure the optimization of the whole system showed in Fig.1.Allowing the improvement of the efficiency maximization.

2 PHOTOVOLTAIC GENERATOR MODELING

Solar cells generate electricity by the direct conversion of the solar energy into electricity. An equivalent circuit model of PV-cell is shown in Fig.2. Cells may be grouped to form panels or modules. Usually a number of PV modules are combined as an array to meet different energy demands. Figure 3 represents the *I-V* and *P-V* characteristics of the PV generator for five insolation levels. The circuit showed in Figure 2 can be represented by (1).

$$I = I_{ph} - I_d - I_{sh} = I_{ph} - I_o\left[\exp\left(\frac{(V+IR_s)}{nA}\right) - 1\right] - \frac{(V+IR_s)}{R_{sh}} \quad (1)$$

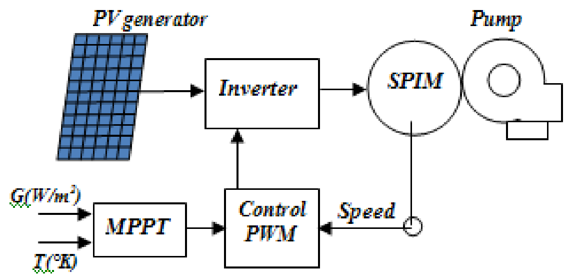

Fig. 1. Block diagram of the global PV pumping system

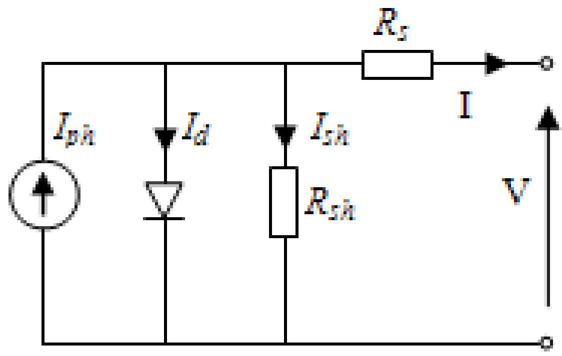

Fig. 2. Solar cell equivalent circuit

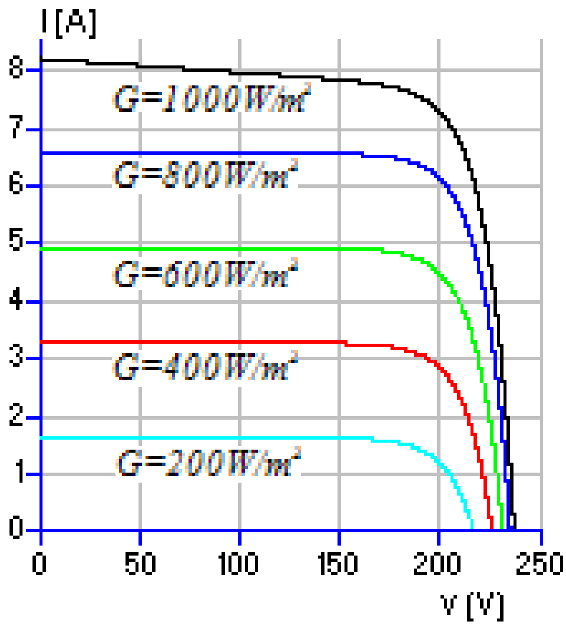

Fig. 3. Characteristics of a PV generator

Where V is the terminal voltage, I is the terminal current, I_{ph} is the solar-generated current, I_d is the diode current, I_o is the diode saturation current, n is the diode ideality constant, R_s is series resistance, R_{sh} is parallel resistance, *A* is the diode quality factor *(A=kT/q).*

Some authors [16], [17], [18] propose the model with four parameters assuming that the parallel resistance R_p is infinite. So the equation (1) is shortened as follows:

$$I = I_{ph} - I_o \left[\exp\left(\frac{q\,(V + R_s I)}{nkT} \right) - 1 \right] \quad (2)$$

$$I_d = I_o \left[\exp\left(\frac{q\,(V + R_s I)}{nkT} \right) - 1 \right] \quad (3)$$

The solar-generated current, I_{ph} linearly depends on solar irradiance and influenced by temperature based on (4), [19-20-21].

$$I_{ph} = \frac{G}{G_n} \left[I_{ph,n} + K_I \left(T - T_n \right) \right] \quad (4)$$

Where $I_{ph,n}$is the solar generated current at the nominal condition (T_n=25°C and G_n=1000W/m^2), *G* is the irradiance, G_n is the nominal irradiance, *T* is the cell temperature, T_n is the nominal cell temperature, K_I is the temperature coefficient at short-circuit.

The diode saturation current, I_o which depends on temperature is given by (5), [20-22].

$$I_o = I_{o,n} \left(\frac{T}{T_n} \right)^3 \exp\left[\frac{qE_g}{nk} \left(\frac{1}{T_n} - \frac{1}{T} \right) \right] \quad (5)$$

Where $I_{o,n}$ is the nominal diode saturation current, *q*=1.60210^{-19} C is the electron charge,*k*=1.380 10^{-23} J/K is the Boltzmann constant, E_g=1.12eV is the bandgap energy.

The current and the voltage parameters of the PV generator are: I_{pv} *= I* and V_{pv} *= ns .Ns.V,* where *ns , Ns* are the number of series cells in panel and series panels in generator(*ns =54*).

Generally, available manufacturer's information are always provide with reference to the nominal condition or standard test conditions (STCs) of temperature and solar irradiation : the nominal open-circuit voltage ($V_{oc,n}$), the nominal short-circuit current ($I_{sc,n}$), the voltage at the maximum power point *MPP* (V_{mp}), the current at the *MPP* (I_{mp}), the temperature coefficient (K_V) at open-circuit and (K_I) at short-circuit.

3 MATHEMATICAL MODEL OF THE SINGLE PHASE INDUCTION MACHINE

Neglecting the core saturation, the dynamic model of single phase induction machines in a stationary reference frame can be represented as [23]:

$$\frac{d\psi_{sd}}{dt} = -R_s i_{sd} + U_{sd} \quad (6)$$

$$\frac{d\psi_{sq}}{dt} = -R_s i_{sq} + U_{sq} \quad (7)$$

$$0 = R_r i_{rd} + \frac{d\psi_{rd}}{dt} + \omega_r \psi_{rq} \quad (8)$$

$$0 = R_r i_{rq} + \frac{d\psi_{rq}}{dt} - \omega_r \psi_{rd} \quad (9)$$

The fluxes are related to the currents by the following equations:

$$\psi_{sd} = L_{sd} i_{sd} + M_{srd} i_{rd} \quad (10)$$

$$\psi_{sq} = L_{sq} i_{sq} + M_{srq} i_{rq} \quad (11)$$

$$\psi_{rd} = L_r i_{rd} + M_{srd} i_{sd} \quad (12)$$

$$\psi_{rq} = L_r i_{rq} + M_{srq} i_{sq} \quad (13)$$

The electromagnetic torque is given by:

$$T_{em} = P \left(M_{srq} i_{sq} i_{rd} - M_{srd} i_{sd} i_{rq} \right) \quad (14)$$

The mechanical equation is:

$$J \frac{d\omega_r}{dt} = \left(T_{em} - T_r - F\omega_r \right) \quad (15)$$

These equations were derived as for an asymmetric two-phase machine [23]. In these equations, variables U_{sd}, U_{sq}, i_{sd}, i_{sq}, i_{rd}, i_{rq}, ψ_{sd}, ψ_{sq}, ψ_{rd} ,ψ_{rq} are auxiliary and main voltages, currents and fluxes of the stator and rotor in the stationary reference frame respectively. R_{sd}, R_{sq} and R_r denote the stator and rotor resistances; L_{sd}, L_{sq}, L_r, M_{srd} and M_{srq} denote the stator, the rotor self, and mutual inductances. ω_r, T_{em}, and T_r are the machine speed, the electromagnetic torque, and the load torque, in this order, and *P, J* and *F* are the machine pole pairs, the moment of inertia, and viscous friction coefficient, respectively.

4 INDIRECT FIELD ORIENTED CONTROL

Note that (6) – (14) are general equations for the two-phase machine. It is seen that there is an asymmetry in the model. This asymmetry is due to the unequal resistances and inductances of the main and auxiliary windings. Since the machine studied is asymmetrical, it can be seen from (14) that the machine produces torque and current oscillations. As was done in [23-24-25] to drive the symmetrical model, here too, the mutual inductances will be employed to define a transformation for the stator variables. This transformation is given by:

$$U'_{sq} = \frac{N_{sd}}{N_{sq}} U_{sq}, \psi'_{sq} = \frac{N_{sd}}{N_{sq}} \psi_{sq}, i'_{sq} = \frac{N_{sq}}{N_{sd}} i_{sq}, \quad (16)$$

In these equations N_{sd}, N_{sq} represent the number of stator windings then the ratio M_{srd}/M_{srq}will be approximately equal to N_{sd}/N_{sq}.Thus, the transformation employed corresponds approximately to refer the auxiliary winding variables to the main winding[14].

The new dynamic model of single phase induction machines in a synchronously rotating reference frame can be described by the following equations:

$$\frac{d\psi_{sd}}{dt} = \omega\psi'_{sq} - R_{sdd}i_{sd} - R_{sdq}i_{sq} + U_{sd} \quad (17)$$

$$\frac{d\psi'_{sq}}{dt} = -\omega\psi_{sd} - R_{sqq}i'_{sq} - R_{sqd}i_{sd} + U_{sq} \quad (18)$$

$$\frac{d\psi_{rd}}{dt} = \omega_{sr}\psi_{rq} - R_r i_{rd} \quad (19)$$

$$\frac{d\psi_{rq}}{dt} = -\omega_{sr}\psi_{rd} - R_r i_{rq} \quad (20)$$

$$\psi_{sd} = L_{sd}i_{sd} + M_{srd}i_{rd} \quad (21)$$

$$\psi_{sq} = L_{sq}i'_{sq} + M_{srq}i_{rq} \quad (22)$$

$$\psi_{rd} = L_r i_{rd} + M_{srd}i_{sd} \quad (23)$$

$$\psi_{rq} = L_r i_{rq} + M_{srq}i_{sq} \quad (24)$$

The new expression of the electromagnetic torque is similar to the one of a symmetrical machine.

$$T_{em} = \frac{P}{L_r}M_{srd}\left(i'_{sq}\psi_{rd} - i_{sd}\psi_{rq}\right) \quad (25)$$

It is noteworthy that the model of the stator flux in (17) and (18) present additional terms that represent the asymmetry of the machine. These terms can be presented in terms of stator windings resistances as:

$$R_{sqq} = \frac{R_{sd} + R'_{sq}}{2} - \frac{R_{sd} - R'_{sq}}{2}\cos(2\theta_{rf}) \quad (26)$$

$$R_{sdd} = \frac{R_{sd} + R'_{sq}}{2} + \frac{R_{sd} - R'_{sq}}{2}\cos(2\theta_{rf}) \quad (27)$$

$$R_{sdq} = R_{sqd} = \frac{R_{sd} - R_{sq}}{2}\sin(2\theta_{rf}) \quad (28)$$

If the magnitude of the variable terms in (26)-(28) is small with respect to the constant terms, the model (17) to (25) becomes symmetric and the conventional rotor-field oriented control strategy can be used [25]

For indirect rotor flux oriented control, the d-axis of the reference frame is oriented along the rotor flux vector which is set be equal to the rated flux, and, consequently, ψ_{dr}=ψ_r and ψ_{qr} =0. After arranging the equations (17) to (24), the mathematical model of single phase induction motor can be represented according to the usual d axis and q axis components in a synchronously rotating rotor flux reference frame as:

$$\frac{M_{srd}}{\tau_r}i_{sd}^{rf} = \frac{\psi_r}{\tau_r} + \frac{d\psi_r}{dt} \quad (29)$$

$$\frac{M_{srq}}{\tau_r}i_{sq}^{\prime rf} = \omega_{sr}\psi_r \quad (30)$$

$$T_{em} = \frac{P}{L_r}M_{srd}\left(i_{sq}^{\prime rf}\psi_r\right) \quad (31)$$

Where ψ_r is the rotor-flux magnitude, ω_{sr}= ω- ω_r is the slip frequency, ω=$d\theta_{rf}$/dt and θ_{rf} are respectively the frequency and the position of the rotor-flux vector.

Expression (31) shows that, if rotor flux is kept constant, i_{sd} can be used to control the flux magnitude and i_{sq} can be used to control the electromagnetic torque.

5 DECOUPLING SYSTEM

In field oriented control of SPIMs, like three phase motors, the stator currents must be controlled. If the employed inverter is of PWM type with voltage control, the voltage command signals should be produced as the outputs of the current controllers. Since it is necessary to calculate the voltage command for a voltage-source inverter, the stator voltage equations for rotor flux control can be derived by (17), (18), (21), (22), (23) and (24):

$$\begin{aligned} U_{sd} = U_d - E_d = \sigma_d L_{sd}\left(\tfrac{1}{\sigma_d\tau_{sd}} + S + \tfrac{(1-\sigma_d)}{\sigma_d\tau_r}\right)i_{sd} \\ - \sigma_q L_{sq}\omega i_{sq} - \tfrac{M_{srd}}{\tau_r L'_r}\psi_r \end{aligned} \quad (32)$$

$$\begin{aligned} U_{sq} = U_q - E_q = \sigma_q L_{sq}\left(\tfrac{1}{\sigma_q\tau_{sq}} + S + \tfrac{(1-\sigma_q)}{\sigma_q\tau_r}\right)i_{sq} \\ +\sigma_d L_{sd}\omega i_{sd} + \tfrac{M_{srq}}{L'_r}\omega_r\psi_r \end{aligned} \quad (33)$$

In these equations τ_{sd} =L_{sd}/R_{sd} , τ_{sq} =L_{sq}/R_{sq},, σ_d=1-M^2_{srd}/(L_r L_{sd}) and σ_q=1-M^2_{srq}/(L_r L_{sq}). E_d and E_q represent the decoupling terms and are given by

$$E_d = \sigma_q L_{sq}\omega i_{sq} + \frac{M_{srd}}{\tau_r L'_r}\psi_r \quad (34)$$

$$E_q = -\sigma_d L_{sd}\omega\, i_{sd} - \frac{M_{srq}}{L_r}\omega_r\psi_r \quad (35)$$

Thus, the dynamics of the d axis and q axis currents are now represented by simple linear first order differential equations. Therefore, it is possible to effectively control the currents with a PI controller. Based on the above equations a synthesis of the decoupling signal is shown in Fig. 4. In Fig. 4, Gd(s) and Gq(s) are the electrical d, q-axis transfer functions of the SPIM. If we assume that the back EMFs is cancelled by the feedforward compensation term, the d, q transfer functions become:

$G_d(S) = \frac{K_d}{1+\tau_d s}$ and $G_q(S) = \frac{K_q}{1+\tau_q s}$

Where K_d=1/R_{sd} and K_q=1/R_{sq} are a static gains and $\tau_d = \tau_{sd}\sigma_d$, $\tau_q = \tau_{sq}\sigma_q$ are a time constants. Also S is a derivation operator.

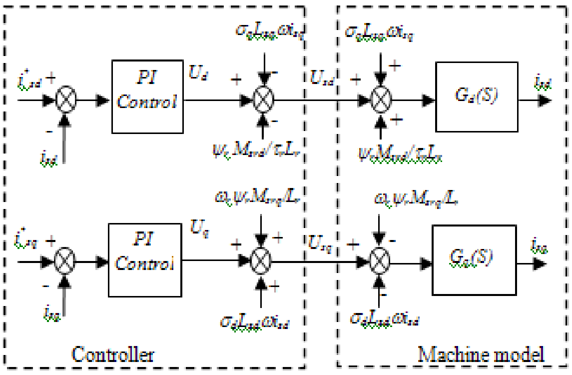

Fig. 4. Decoupling with compensation terms

Fig. 5 shows the block diagram of the indirect rotor-field-oriented control scheme, which has been adapted for the single-phase machine. In this diagram T^*_{em} and $\psi^*{}_r$ represent the reference electromagnetic torque and amplitude of the rotor flux, respectively. Block $e^{j\theta rf}$ performs the coordinate transformation from the reference frame aligned along with the rotor-flux vector to the stationary reference frame. Blocks *PI control* represent the speed controller, d and q-axis current controller respectively. It is seen that the two current controllers provide control voltages U_d and U_q. These voltages are supplemented by decoupling voltages E_d and E_q respectively to produce voltages commands. Block PVG, *PWM INVERTER* and *SPIM* represent the photovoltaic generator, the voltage-source inverter and the single phase induction machine pump. In order to calculate the reference speed, we use a sensor in order to measure the illumination value and a calculator to deduce the reference speed *via* the MPPT.

6 CENTRIFUGAL PUMP MODEL

The centrifugal pump is described by an H (Q) characteristic given by [26], [27]. The multispeed family head-capacity curves are shown in Fig. 6 and can be expressed approximately by the following quadratic form:

$$H = c_0\omega_r^2 - c_1\omega_r Q - c_2 Q^2 \tag{36}$$

Where c_0,c_1 and c_2 are constant parameters.

The hydrodynamic load torque of the centrifugal pump is given by the following equation [9]

$$P_H = \rho g Q H, \tag{37}$$

Where Q is the water flow (m^3/s), H is the manometric head of the well (m), ρ the density (Kg/m^2) and g the gravity (m/s^2).

The centrifugal pump load torque T_r is assumed to be proportional to the square of the rotor speed:

$$T_r = A_p\omega_r^2 \tag{38}$$

Where A_p is the torque constant ($A_p = \frac{P_n}{\omega_n^3}$), P_n is the nominal power of the single phase induction motor and ω_n is the rotor nominal speed.

7 PROPOSED APPROACH

By neglecting frictions and losses, we can express the power of the single phase induction motor as follows:

$$T_r\omega_r = A_p\omega_r^3 \tag{39}$$

The maximum input power can be expressed as:

$$P_{mp} = \frac{A_p\omega_{opt}^3}{\eta} \tag{40}$$

Where P_{mp}, η are the maximum input power and motor efficiency. In nominal conditions of insulation and temperature we have:

$$P_n = \frac{A_p\omega_n^3}{\eta} \tag{41}$$

Where P_n, η, ω_n, are the nominal values of input power, speed and efficiency of the motor in nominal conditions. From (40) and (41), we can define the new optimal speed according to the optimal power of photovoltaic generator. This is the control reference speed of the speed control loop, as shown in fig.5

$$\omega_{opt} = \omega_n\sqrt[3]{\frac{P_{opt}}{P_n}} \tag{42}$$

Where $P_{opt=}\ P_{mp.}\ \eta$

The following table represents the reference speed and the optimal PV power for different values of the solar illumination.

Table 1. Reference speed and PV power versus the illumination value

G(W/m^2)	P_{opt}(W)	ω_{opt} (rad/s)
100	125	72.53
200	275	94.33
300	426	109.15
400	576	120.7
500	742	131.33
600	815	135.5
700	1059	147.86
800	1106	150.02
900	1386	161.74
1000	1453	164.30

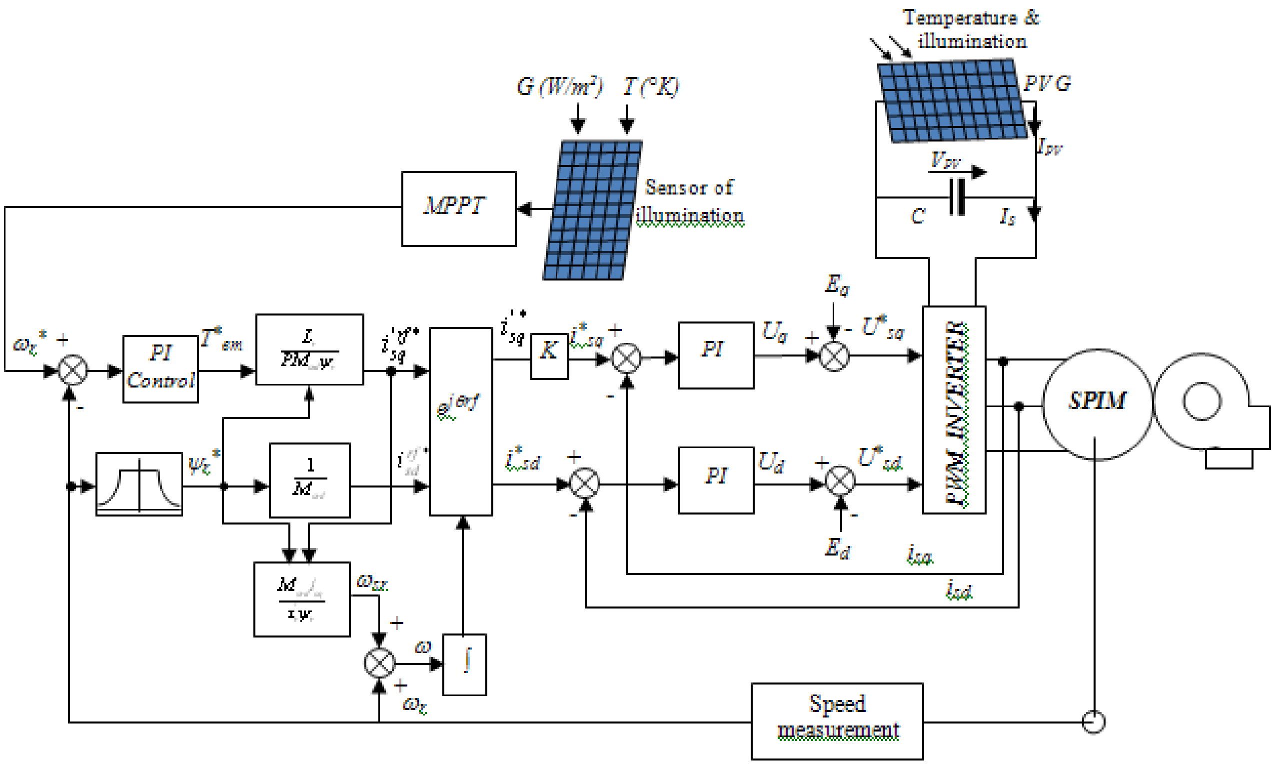

Fig. 5. Block diagram of the indirect rotor flux control system and the PVG

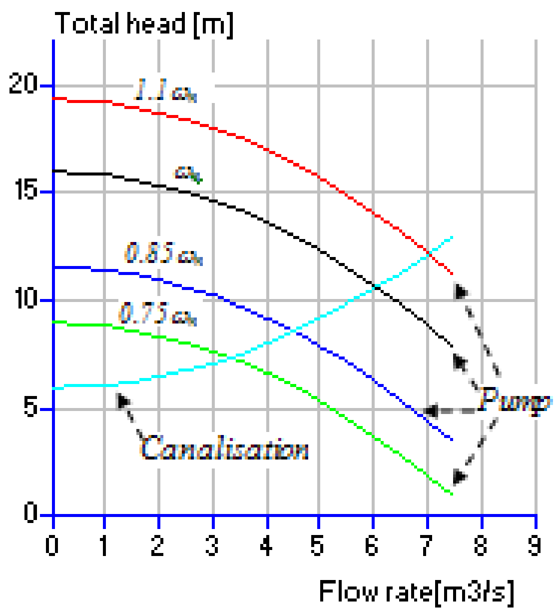

Fig. 6. Flow rate characteristic

8 SIMULATION RESULTS

In order to demonstrate the effectiveness of the proposed control technique applied to the photovoltaic water pumping system, some simulations have been carried out. The proposed design scheme is described by Fig. 5.

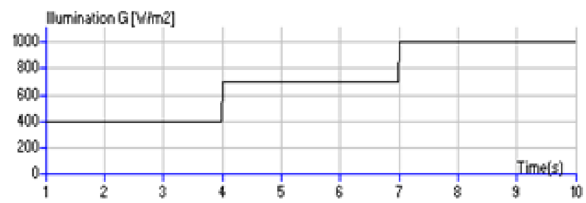

Fig. 7. The solar illumination waveform

In the first step, we choose to vary the solar illumination value G as it is shown in Fig. 7, and to see its impact on the performances of the photovoltaic water pumping.

Fig. 8a, illustrates the waveform of the mechanical speed of the induction motor which is close to its optimal value determined by equation (42).

The same remark is given to the electromagnetic torque shown by Fig. 8b. It is clearly shown that the induction motor is operating at its optimal conditions.

Fig.8c represents the waveform of the centrifugal pump flow which is close to its optimal value for each value of illumination.

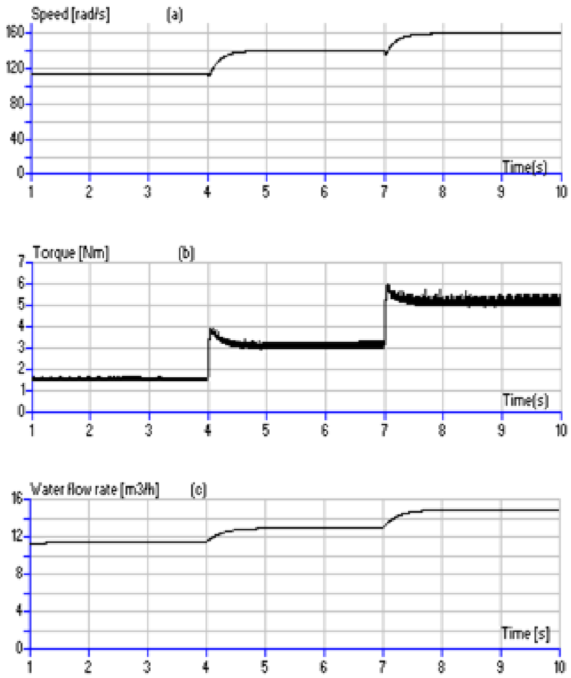

Fig. 8. Response of the system to the variation of illumination G

In the second step, a comparative study on system performances is carried out on two systems: direct coupled and the optimized.

Fig.9 shows the operating point displacement of a SPIM-Centrifugal pump supplied by photovoltaic generator for different levels of solar insulation. The maximum power and optimal voltages are also shown. It is seen that, depending on the load (Power -Voltage) characteristic, a directly connected motor-photovoltaic system with a given load characteristic can be naturally optimized at the intersection point of the load characteristic and maximum power locus. We notice also in this case that the photovoltaic water pumping system operation points curve corresponding to the optimized system is shifted towards the maximum electric power points of the PV generator (curve P(V)), which ranges between 180 and 220 volts, for a variable illumination levels between 200W/m^2 and 1000W/m^2 (see Fig.9). It is clearly seen that the performance of the pumping system is improved if the output power of the photovoltaic generator is optimal. This result has motivated the use only of an inverter in order to force the PVG to operate at its maximum power point under different solar illumination conditions.

Figure 10 represents the speed versus the solar illumination intensity. We note a speed increase of the optimized system with the illumination intensity increasing (see Fig. 10).Moreover, for an insolation of 605 W/m^2 the optimized and non-optimized speed coincide, this means that the group SPIM-centrifugal pump is well adapted to the PVG at this insolation level. For the direct coupling the driving system motor- pump may stay at standstill until the solar insolation is sufficiently high to develop the required torque for starting. Therefore, it starts to rotate only at G=274W/m^2, contrary to the optimized coupling the system starts to rotate at lower insolation level G=98W/m^2

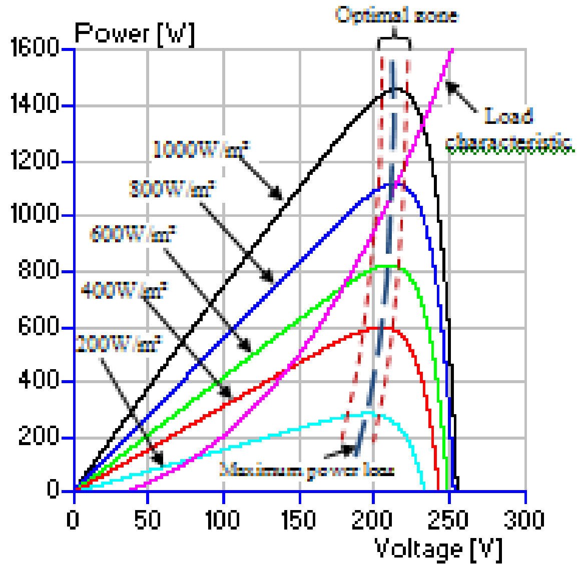

Fig. 9. Operation points of the photovoltaic pumping system driven by a SPIM

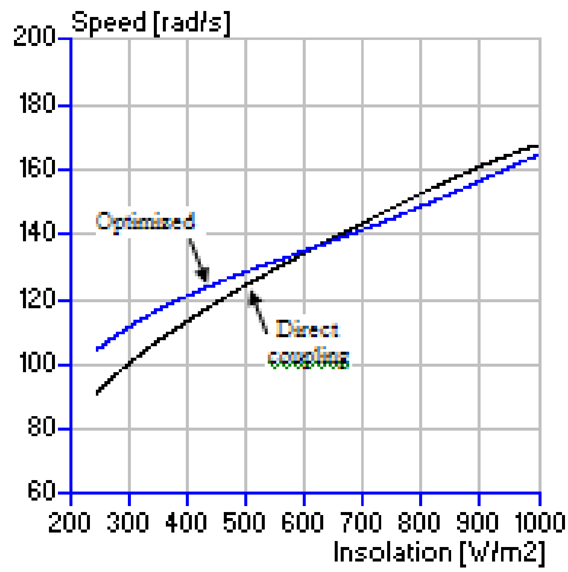

Fig. 10. Speed of the photovoltaic pumping after and before optimization

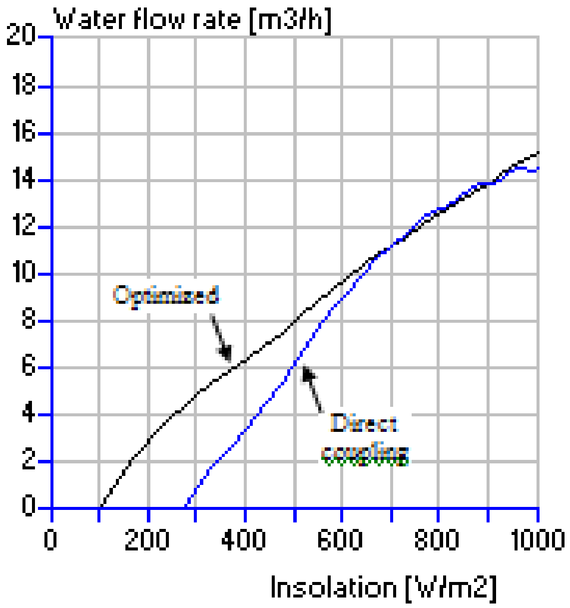

Fig. 11. Flow rate of the photovoltaic pumping system driven by a SPIM

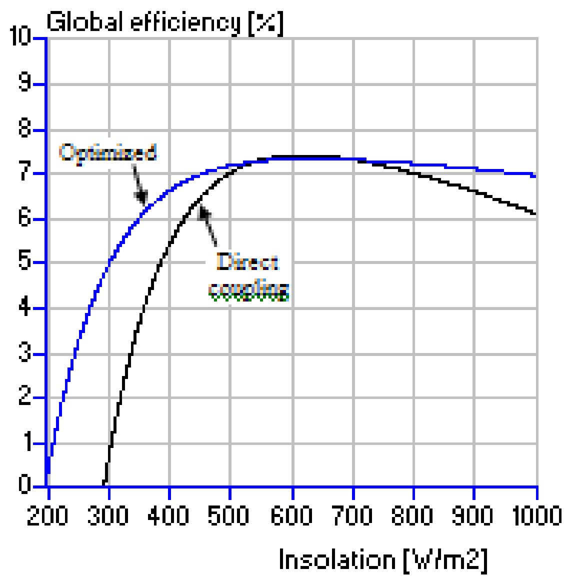

Fig. 12. Global efficiency of the photovoltaic pumping system driven by a SPIM

(see Figs. 11 and 12). The Fig. 12 represents the global efficiency versus the solar illumination intensity, of the photovoltaic pumping systems. Optimization is better for weak illuminations, until G=530W/m^2, the global efficiency of the photovoltaic pumping system driven by a SPIM being weak, approximately between 7% and 7.5%. But, it can be noted that the system global efficiency is improved by the proposed MPPT method.

9 CONCLUSION

In this paper the performances of a photovoltaic pumping system driven by a single phase induction motor (SPIM) coupled to a centrifugal pump is proposed. The main concluding remarks are summarized as follows:

The obtained simulation results have shown the good performance of the proposed algorithm MPPT in terms of global efficiency optimization of the PV water pumping system, and water discharge rates in the steady state operation. Furthermore, the effectiveness of the drive system for both, steady state, transient and severe solar insolation variations, was also shown.

We have proved the utility of the chosen MPPT method in optimization of the photovoltaic pumping system performances.

It is shown that the concept of the indirect rotor-field-oriented control (IRFOC) techniques is used to pilot the working of the single phase induction motor coupled the centrifugal pump. This method makes it possible to obtain very good performances similar to those of a DC motor.

It is shown also via this paper, that the performance of the pumping system is improved if the output power of the photovoltaic generator is optimal; this result has motivated the use only of an inverter in order to force the PVG to operate at its maximum power point under different solar illumination conditions.

Finally, considering the robust, maintenance free and low cost characteristics of single phase induction motors, it is evident that SPIM based PV water pumping systems will become very popular in the near future. The next stage of this work is the experimental validation in order to checking the analytical results obtained.

APPENDIX

The parameters of single phase induction machine

Power:1.1kW, Voltage:230V , Current:7.6A
Frequency:50Hz , Speed:1430 rpm , Number of pole pairs:2
R_{sd}=2.4Ω, R_{sq}=5.66Ω, R_r =6.161Ω
M_{srd}=0.0829H, M_{srq}=0.0990H, L_{sd}=0.0909H
L_{sq}=0.1150H, L_r=0.0915H
J=5.83.10^{-3}Kg.m^2, f=2.02.10^{-4}N.m.s.rad^{-1}

PVG parameters

P_{mp}=200W, V_{mp}=26.3V, I_{mp}=7.61A, $V_{oc,n}$=32.9V, $I_{cs,n}$=8.21A
G_{ref} =1000W/m^2, K_V= -0.123 A/°C, K_I= 0.00318 A/°C, N_s=54, N_p=7

Centrifugal pump parameters

ω_n = 150 rad/s, c_0 = 4.9234 10^{-3} m/(rad/s)^2, c_1 = 1.5826 10^{-5} m/(rad/s)(m^2/s), c_2 = -18144 m/(m^3/s)^2, Q=15 m^3/h, H=20 m

REFERENCES

[1] M. Kolhe, and J. C. Joshi1, "Performance analysis of directly coupled photovoltaic electro-mechanical systems," Proceedings *of the Institution of Mechanical Engineers, Part A: Journal of Power and Energy,* 216, pp. 453-463, 2002.

[2] J. Appelbaum, and M. S. Sarma, "The operation of permanent magnet DC motors powered by a common source of solar cells," *IEEE Trans Energy Convers,* vol.4 no.4, 635-642, 1989.

[3] S.I. Singer, and J.Appelbaum, "Starting characteristics of direct current motors powered by solar cells," *IEEE Transactions on Energy Conversion,* vol.8, no.1, pp.47-53, 1993.

[4] C. L. Putta Swamy, B. Singh, and B. P. Singh, "Dynamic Performance of a Permanent Magnet brushless DC Motor Powered by a PV Array for Water Pumping," *Solar Energy Materials Solar Cells,* vol.36, pp. 187-200, 1995.

[5] S. R. Baht, A. Pittet, and B. S. Sonde, Performance Optimisation of Induction Motor-Pump using Photovoltaic Energy Source*, IEEE Trans Ind App*, vol.23 no. 6, 995-1000, 1987.

[6] M. F. Mimouni, M. N. Mansouri, B. Benghanem, and M. Annabi, "Vectorial command of an asynchronous motor fed by a photovoltaic generator," *Renewable Energy*, vol.29, pp. 433-442, 2004.

[7] A-K. Daud, and M. Mahmoud, "Solar Powered Induction Motor Driven Water Pump Operating on a Desert Well, Simulation and Field Tests," *Renewable Energy,* vol.30, pp. 701-714, 2005.

[8] E. Muljadi, "PV Water Pumping with a Peak Power Tracker using a Simple Six Step Square-Wave Inverter," *IEEE Trans. Industry Applications,* vol.33 no. 3, pp.714-721, 1997.

[9] M. Arrouf, and N. Bouguechal "Vector control of an induction motor fed by a photovoltaic generator," *Applied Energy,* vol.74, pp.159-167, 2003.

[10] Y. Weslati, A. Sallemi, F. Bacha, and R. Andoulsi, "Sliding mode control of a photovoltaic grid connected system," *Journal of Electrical Systems,* ISSN 1112-5209,.vol.4, issue 3, 2008.

[11] H. Tarik Duru, "A maximum power tracking algorithm based on Impp=f(Pmax) function for matching passive and active loads to a photovoltaic generator," *Solar Energy*, vol.80, pp. 812-822, 2006.

[12] D. H. Jang, and D. Y. Yoon, "Space-vector PWM technique for two-phase inverter-fed two phase induction motors," *IEEE Trans. Ind. Appl,* vol.39, no. 2, pp. 542–549, 2003.

[13] M. A. Jabbar, A. M. Khambadkone, and Z. Yanfeng, "Space-vector modulation in a two-phase induction motor drive for constant-power operation," *IEEE Trans. Ind. Electron.*, 51, no. 5, pp. 1081-1088, 2004.

[14] M. B. R. Correrea, C. B. Jacobina, A.M. N. Lima, and E. R. C. Dasilva, "A three-leg voltage source inverter for two-phase AC motor drive systems," *IEEE Trans. Power Electron.*, vol.17, no. 4, pp. 517-523, 2002.

[15] F. Blaabjerg, F. Lungeanu, K. Skaug, and M. Tonnes, "Two-phase induction motor drives," *IEEE Trans. Ind. Appl.Mag.*, vol.10, no. 4, pp. 24-32, 2004.

[16] M. Veerachary, "PSIM circuit-oriented simulator model for the nonlinear photovoltaic sources," *IEEE Trans. Aerosp. Electron. Syst.*, vol.42, no. 2, pp. 735-740, 2006.

[17] W. Xiao, W. G. Dunford, and A. Capel, "A novel modeling method for photovoltaic cells," *in Proc. IEEE 35th Annu. Power Electron. Spec. Conf. (PESC)*, vol. 3, pp. 1950-1956, 2004.

[18] E. Matagne, R. Chenni, and R. ElBachtiri, "A photovoltaic cell model based on nominal data only," *in Proc. Int. Conf. Power Eng., Energy Elect. Drives, Power Eng*, pp. 562-565, 2007.

[19] D. Sera, R. Teodorescu, and P. Rodriguez, "PV panel model based on datasheet values," *in Proc. IEEE Int. Symp. Ind. Electron. (ISIE)*, pp. 2392-2396, 2007.

[20] W. De Soto, S.A. Klein, and W.A. Beckman, "Improvement and validation of a model for photovoltaic array performance," *Solar Energy*, vol.80, no. 1, pp.78-88, 2006.

[21] A. Driesse, S. Harrison, and P. Jain, "Evaluating the effectiveness of maximum power point tracking methods in photovoltaic power systems using array performance models," *in Proc. IEEE Power Electron. Spec. Conf. (PESC),* pp. 145-151, 2007.

[22] Q. Kou, S. A. Klein, and W. A. Beckman, "A method for estimating the long-term performance of direct-coupled PV pumping systems," *Solar Energy*, vol.64, no. 1-3, pp.33-40, 1998.

[23] P. C. Krause, O. Wasynczuk and S. D. Sudhoff "Analysis of Electric Machinery and Drive Systems," John Wiley and Sons, NewYork, 2002.

[24] C-E. Feraga, A. Bouldjedri, "Indirect rotor field oriented control strategy for single phase induction motor drives," *Przeglad elektrotechniczny (electricalreview),* vol.88, pp.222-225, 2012.

[25] S. Vaez-Zadeh, S.H. Reicy, "Decoupling vector control of single-phase induction motor drives," *36^{th} Power Electronics Specialists Conference PESC*, pp.733-738, 2005.

[26] A. Moussi, A. Betka, B. Azoui, "Optimum design of photovoltaic pumping system," *Leicester, UK: UPEC99*, 1999.

[27] A. Hamidat, A. Hadj arab, F. Chenlo, M. A. Abella, Performances costs of the centrifugal and displacement pumps," *World Renewable Energy Congress, Florence Italy,WREC V,* pp.1951-1954, 1998.

C. Feraga was born in 1969, in Algeria. He received the Engineer degree, the Magister degree and the Doctorat d'Etat (PhD) in Electrotechnics, from the University Badji Mokhtar of Annaba, Algeria, in 1994, 1998 and 2009 respectively. In 1999, he joined the Electrical Engineering Department of Guelma University. He is currently Associate Professor of Electrical Engineering Department at the University of Guelma, and his research interests are in the area of electrical drives power electronics and renewable energies.

A. Bouldjedri was born in 1967, in Algeria. He received the Engineer degree from university of Boumerdès, Algiers, Algeria, in 1990 and the Magister degree in Electrotechnics, from the University of Annaba, Algeria, in 1999.In 1991, he joined the Electrical Engineering Department of Sonatrach Company, Algeria. He is currently preparing his PhD thesis on a topic of power system at the Department of Electrical Engineering, University Badji Mokhtar of Annaba, Algeria. He is currently a member of electrical engineering Department at Sonatrach Company, and his research interests are in the area of electrical drives, process control, power system and renewable energies.

AUTHORS' ADDRESSES

Assoc. Prof. Chams-Eddine Feraga, Ph.D.
Department of Electrical Engineering, and Automatic,
Faculty of Science and Technology,
University of 8 May 1945 of Guelma,
BP 401, Guelma 24000, Algeria.
Laboratory of Electrical Engineering (LGEG),
University of 8 may 1945 of Guelma, Guelma 24000, Algeria.
Email: chferaga@yahoo.fr

Abdallah Bouldjedri, M.Sc.,
Department of Electrical Engineering,
Sonatrach Company, Ouargla 30000, Algeria
Email: b_abj67@yahoo.fr

Received: 2014-04-28
Accepted: 2015-01-21